

# A Study on effect of thermal treatment on crystalline Properties of Microwave Assisted Synthesized TiO<sub>2</sub>

Ruby Gill<sup>1</sup>, Prem Prabhakar<sup>2</sup>, Mukti Sharma<sup>3</sup>, Pushpendra Kumar<sup>3\*</sup>

<sup>1</sup>Department of Chemistry, Lovely Professional University, Punjab

<sup>2</sup>Department of Chemistry, Paliwal Degree College Shikohabad, Firozabad

<sup>3</sup>Department of Chemistry, J. S. University, Shikohabad

\*Corresponding author: Email: [pushpendra.kmr1@gmail.com](mailto:pushpendra.kmr1@gmail.com)

## Abstract:

In the present study, Titanium Dioxide (TiO<sub>2</sub>) was prepared by microwave assisted sol-gel synthetic method and effect of heat treatment on microcrystalline properties was studied. Synthesized material was sintered at three different temperature; 400, 500 and 600 °C. To investigate microstructural properties, samples were introduced to X-Ray diffraction (XRD), scanning electron microscopy (SEM), Energy dispersive spectroscopy (EDS) UV-Visible spectroscopy. XRD pattern depicts semicrystalline behaviour of unannealed TiO<sub>2</sub> which was converted into perfect crystalline nature at higher thermal treatment. Exhaustive growth of tetragonal anatase phase of TiO<sub>2</sub> was observed. However, the TiO<sub>2</sub> annealed at 600 °C traces of rutile phase was also observed which reflects phase transformation at higher annealing temperature. The absorption spectra shows that all the samples are UV active as they absorb UV radiation strongly. FE-SEM images shows clusters of spherical particles in the range of 20-30 nm.

**Keywords:** TiO<sub>2</sub>, microcrystalline properties, thermal treatment

## Introduction:

TiO<sub>2</sub> has been widely used in various catalytic activities especially in light assisted photocatalysis due to its excellent features like inexpensive, non-toxic, stable under illumination, chemically and biologically inert, resistant to photocorrosion and easy to synthesize [1]. It has been used in many applications like sensors, water purifications, medicine, cosmetics, solar cell and energy harvesting devices [2-4]. TiO<sub>2</sub> has been extensively investigated for photocatalytic degradation of Volatile organic compounds, catalytic hydrogen production and cosmetic products as it has n-type character having high charge carrier mobility and high oxidising power.

TiO<sub>2</sub> exists in three crystalline phases (i) Tetragonal Anatase (ii) Tetragonal Rutile and (iii) Orthorhombic Brookite [5]. Out of three distinct phases of TiO<sub>2</sub>, tetragonal anatase phase having low charge carriers recombination rate shows better activity compared to other two phases and is a most stable polymorph.

Properties of material not only depend on its chemical composition but also on size, morphology and topography of the respective material. Nanostructures like nanoparticles, Nanospheres, nanorods, nanotubes, nanofibers etc. show different activities due to different effective exposed surface area, morphology, defects which in turn affects the charge carrier

recombination rate determining the overall efficiency of the process [6]. Nanotechnology has emerged as a tailoring tool to modify the properties of the material. By changing the size and morphology of any material, its reactive surface area, charge transport length and charge recombination rate may be modified. For each application, specific phase composition, morphology and reactive surface area is required which can be obtained by using nanotechnology especially at material synthesis level [7]. TiO<sub>2</sub> may show mesoporous structure based on size distribution which may vary based on its synthetic conditions. Its band gap also depends on structure and may vary with change in crystalline size and structure.

Many Physical and chemical methods have been adopted to synthesize TiO<sub>2</sub> but sol-gel method has advantages over other like low cost, easy to handle, chemical homogeneity and composition may be altered at molecular level [8]. This method may be co-linked by other physical techniques like hydrothermal, ultrasonication, solvothermal and many others. However, sol-gel method takes large time for completion of reaction which may lead to contamination. Microwave assisted sol-gel synthesis has advantage over conventional sol-gel process as it provide quick, even and energy efficient heating resulting in much less reaction time reducing the cost and energy requirement of the process [9].

In this study, TiO<sub>2</sub> was synthesized by microwave assisted Sol-Gel route and was subjected to anneal at different annealing temperature to analyse the effect of annealing temperature on crystalline structure of TiO<sub>2</sub> and on its antibacterial & antifungal activity.

### **Experimental:**

To make TiO<sub>2</sub> sol, equimolar amount of TiCl<sub>4</sub> and hexamethylenetetramine was mixed in double distilled water and stirred for 15 minutes. Solution was transferred in screw tight bottle and was kept in microwave oven at 250 °C for 15 minutes. Precipitate was filtered and washed with water for several times. Precipitate was dried in oven followed by annealing at 400, 500 and 600 °C and samples are symbolized as T4, T5, T6, respectively. Unannealed sample is symbolized as T.

Crystalline size and phase was determined by X-Ray diffraction (Bruker D8 Advance) by using CuK $\alpha$  radiation of wavelength 1.54 Å. Morphological studies were done by using FE-SEM (JEOL JSM-7610F Plus). Particle size distribution was analysed by particle size analyser (Malvern Zetasizer Nano ZS90). Samples were also subjected to UV-Visible.

### **Results and Discussion:**

Nanostructured TiO<sub>2</sub> was synthesized successfully by a microwave assisted sol-gel route. Unlike conventional methods, microwave irradiation reduced the reaction time and sufficient precipitation was observed within 15 minutes. Density of samples varied from 3.23 – 3.88 g/cm<sup>3</sup> which is less compared to standard density of TiO<sub>2</sub> which shows that as synthesized TiO<sub>2</sub> is highly porous.

Figure 1 shows the X-Ray diffraction pattern of TiO<sub>2</sub> annealed at different temperature. In case of unannealed TiO<sub>2</sub> very less intense and broad peaks were recorded indicating semicrystalline nature of TiO<sub>2</sub>. XRD peak at 2 $\theta$  25.30 corresponds to TiO<sub>2</sub> but other peaks are very less intense to be recognized. For better crystallinity, TiO<sub>2</sub> was annealed at 400 °C under air. Exhaustive evolution of tetragonal Anatase phase of TiO<sub>2</sub> was observed and presence of multiple peaks indicates polycrystalline nature of TiO<sub>2</sub>. Peaks at 2 $\theta$  25.35, 37.82, 48.06, 54.08, 55.15, 62.77 and 68.89 corresponding to the planes (101), (004), (200), (105), (211), (204) and (116), respectively confirms the anatase phase of TiO<sub>2</sub> (PDF00-064-0863).

No peak corresponding to rutile or brookite phase of  $\text{TiO}_2$  was observed. Crystalline size was determined by Scherrer's calculation by using FWHM and Integral breadth of XRD peaks and the values are given in table 1. Highly intense peaks compared to unannealed  $\text{TiO}_2$  indicates better crystallinity of  $\text{TiO}_2$  as at higher temperature atoms get enough thermal energy to occupy proper sites in crystal lattice leading better crystallization. As the annealing temperature was increased to  $500^\circ\text{C}$ , two additional low intense peaks were observed at  $2\theta$   $36.8^\circ$  and  $38.6^\circ$  corresponding to plane (103) and (112). As the temperature increases, more thermal energy is provided to atoms to get them oriented along particular stable orientation. In XRD plots, it can be seen that on increasing annealing temperature, intensity of peak corresponding to plane (101) increased significantly while intensity of other peaks decreased. This shows that at  $400^\circ\text{C}$  crystals are oriented along all planes but on increasing annealing temperature orientation of crystals is favoured along (101) plane. On further increasing annealing temperature to  $600^\circ\text{C}$ , very interesting fact was observed i.e phase transition. When samples were annealed at  $600^\circ\text{C}$ , along with anatase phase, presence of rutile phase was also observed. Additional peaks at  $2\theta$   $27.5$ ,  $36.1$ ,  $41.2$ ,  $44$ ,  $54.5$ ,  $56.6$  and  $64.2$  corresponding to the plane (110), (101), (111), (210), (211), (220) and (310) planes of rutile  $\text{TiO}_2$  (PDF 01-086-0147). Generally rutile phase is more stable in bulk  $\text{TiO}_2$  but in case sol-gel processed  $\text{TiO}_2$  anatase phase is preferred. Transition of anatase phase to rutile generally occur at higher temperature but also depends upon the synthetic conditions and chemicals used [10]. Different studies show transition of anatase to rutile at different temperature [11]. In this study we observed phase transition at lower temperature compared to other reported phase transition temperature. Intensity of peak corresponding to plane (101) is high compared to other peaks which indicate that preferred orientation was restored even on increasing the temperature to  $600^\circ\text{C}$ . Microscopic details of samples calculated by XRD data is given in table 1 (only major peaks are considered). From the table 1 it can be seen that as the annealing temperature was increased, crystalline size also shifted towards higher side which is in well agreement with XRD pattern as on increasing the annealing temperature, intensity of major peaks increased due to better crystallinity [12].

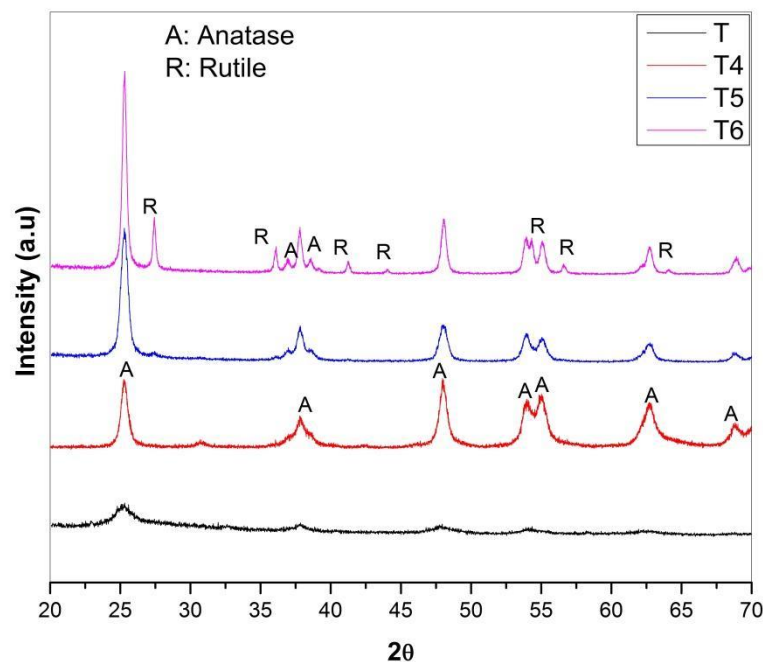


**Figure1:** X-Ray diffraction pattern of  $\text{TiO}_2$  at different annealing temperature

**Table 1: Microscopic details of TiO<sub>2</sub> annealed at different temperature**

Sample	Peak position	FWHM	Integral breadth (IB)	Crystalline Size		d spacing	Average Particle size (d.nm)	PDI
				By using FWHM	By using IB			
T	25.3	1.282	1.511	7	6	3.50953	192.4	0.255
	37.8	0.509	0.717	16	12	2.37743		
	47.8	0.737	0.981	12	9	1.89764		
	54.1	0.435	0.686	20	13	1.69152		
	62.8	0.846	0.540	11	17	1.47713		
T4	25.3	0.546	0.667	15	12	3.52350	828.1	0.387
	37.8	0.754	1.043	11	8	2.37501		
	48.0	0.616	0.718	14	12	1.89362		
	62.7	0.972	1.284	11	8	1.47996		
T5	25.3	0.582	0.664	14	12	3.51456	734	0.634
	37.8	0.441	0.418	19	20	2.37743		
	47.9	0.680	0.708	13	12	1.89214		
	53.9	0.534	0.610	17	15	1.69687		
	55.0	0.430	0.442	23	23	1.66636		
	62.8	0.732	0.828	14	13	1.48026		
T6	25.3	0.364	0.423	23	19	3.50877	819.6	0.643
	27.4	0.226	0.266	37	31	3.24698		
	36.0	0.233	0.258	36	33	2.48669		
	37.8	0.299	0.332	31	28	2.37690		
	41.3	0.196	0.220	48	43	2.18768		
	48.1	0.415	0.468	23	21	1.89003		
	53.9	-	-	-	-	1.69806		
	55.1	0.352	0.360	28	28	1.66401		
	54.3	-	-	-	-	1.68781		
	62.7	0.439	0.580	24	18	1.47993		

To investigate the optical properties, absorbance of TiO<sub>2</sub> annealed at different temperature was recorded by UV-Visible spectrophotometer. Figure 2 shows the absorption curves of different samples. All the samples shows significant absorption in UV region. Band gap is a bulk property so all the samples shows almost similar  $\lambda_{max}$ . However, optical absorption varied with increase in annealing temperature. Unannealed TiO<sub>2</sub> showed lower optical absorption and TiO<sub>2</sub> annealed at higher temperature showed better optical absorption.

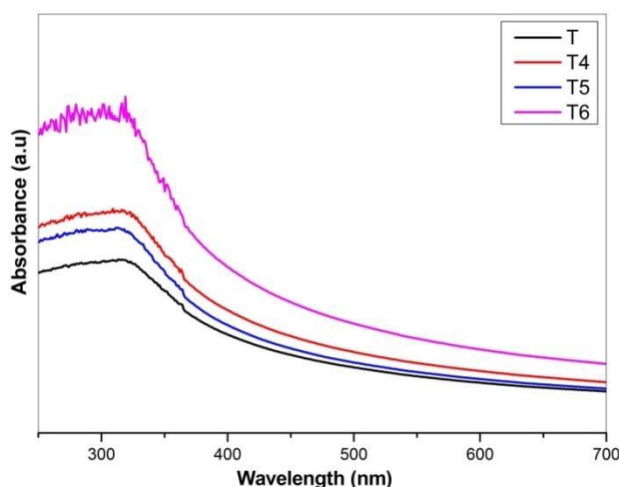


**Figure2:** Absorbance vs wavelength curves of TiO<sub>2</sub> annealed at different temperature

TiO<sub>2</sub> annealed at 400 and 500 °C showed almost same absorption but TiO<sub>2</sub> annealed at 600°C showed much better optical absorption with little redshift compared to other samples. This rise in optical absorption may be attributed to improved crystallinity at higher annealing temperature[13]. It is known that as the crystalline size increases, band gap reduces and hence, red shift in sample T6 can be seen.

Dynamic light scattering (DLS) study was done by using particle size analyser which works on Brownian motion of particle in dispersed solution and based on light scattering by suspended particle determines the particle size of respective material. Prepared TiO<sub>2</sub> samples were dispersed in ethanol and sonicated for 30 minutes. Obtained values of average particle size in d.nm and Polydispersity Index (PDI) are depicted in table 1 along with Poly dispersity index (PDI). Figure 3A and 3B shows size distribution curve obtained as such by zetasizer for unannealed TiO<sub>2</sub> and TiO<sub>2</sub> annealed at 600°C

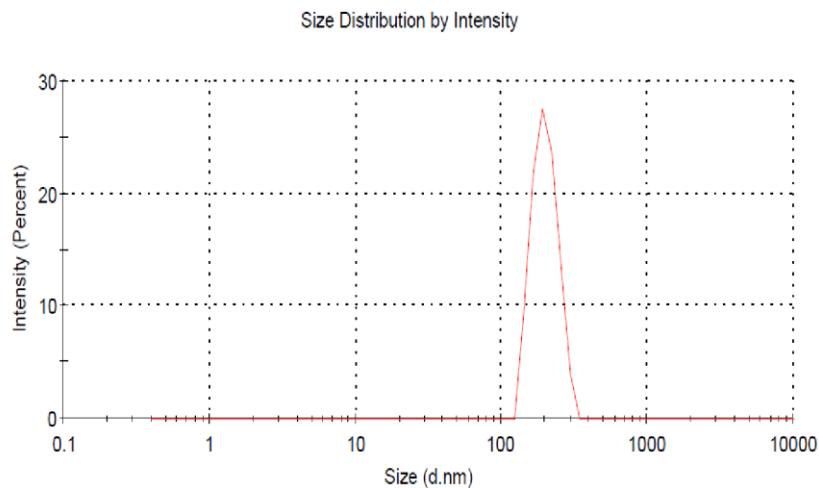


**Figure 3(A):**Size distribution curve of Unannealed TiO<sub>2</sub> (T)

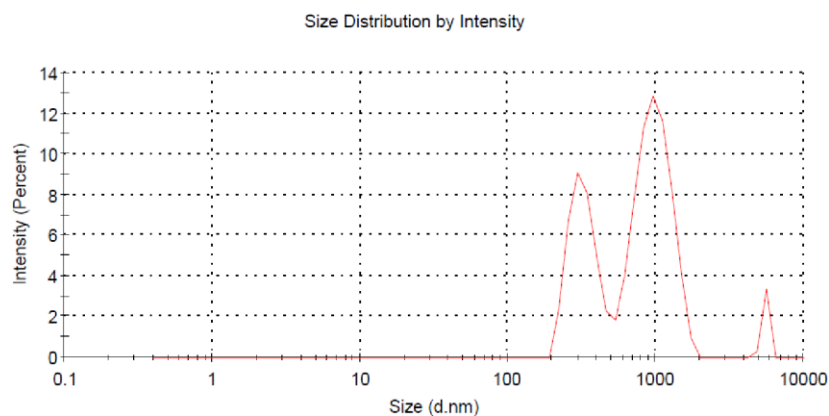


**Figure 3(B):** Size distribution curve of TiO<sub>2</sub> annealed at 600 °C (T6)

To find out the effect of annealing temperature on morphology of TiO<sub>2</sub>, samples were subjected to FE-SEM equipped with EDS measurements. Figure 4 shows FE-SEM images of

TiO<sub>2</sub> annealed at different temperatures. SEM images depict cluster appearance due to agglomeration of particles with irregular crystalline morphology having size in the range 20-30 nm. In samples annealed at higher temperature, clear grain boundaries can be seen and crystalline size match with that of calculated by XRD. In case of sample T6, particle size lower than 30 nm with clear grain boundaries having uniform morphology can be seen.

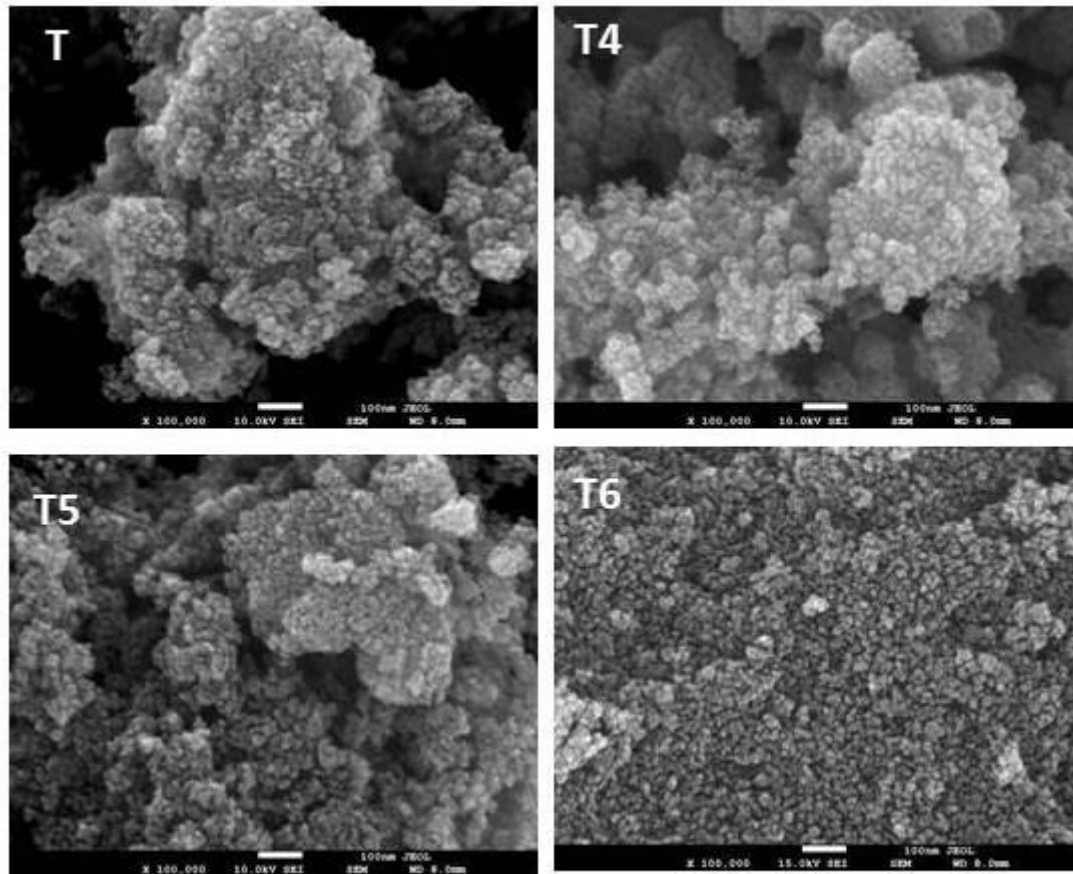


**Figure 4:**FE-SEM images of TiO<sub>2</sub> annealed at different temperature

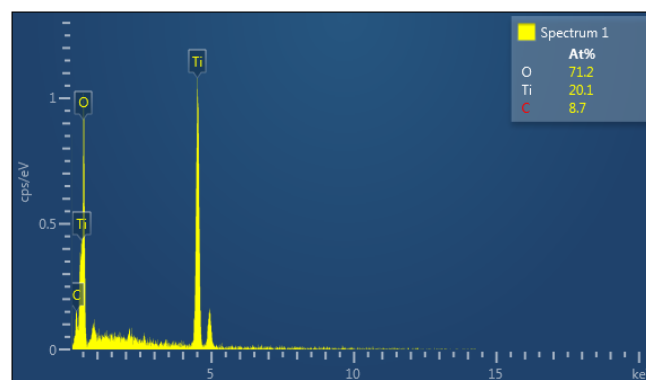


**Figure 5:**EDS measurement of TiO<sub>2</sub> annealed at 600°C (T6)

Elemental composition of synthesized TiO<sub>2</sub> annealed at 600 °C is shown in figure 5 which confirms the presence of Titanium and oxygen. Additional peak corresponding to carbon is due to carbon tape used during the EDS measurement.

**Conclusion:** Nanostructured TiO<sub>2</sub> was synthesized successfully by microwave assisted sol-gel route and annealed at different temperature. On annealing dominant evolution of anatase phase of TiO<sub>2</sub> was observed. On annealing at 600 °C, along with anatase phase, rutile phase of TiO<sub>2</sub> was also observed indicating phase transition of anatase to rutile.

## References

1. K.B. Chaudhari, Y.N. Rane, D.A. Shende, N.M. Gosavi and S.R. Gosavi, Effect of annealing on the photocatalytic activity of chemically prepared TiO<sub>2</sub> thin films under visible light, *Optik - International Journal for Light and Electron Optics*, Vol.193, pp.163006 (2019)
2. Prateek Bindra and Arnab Hazra, Selective detection of organic vapors using TiO<sub>2</sub> nanotubes based single sensor at room temperature, *Sensors and Actuators B: Chemical*, Vol.290, pp. 684-690, (2019).
3. Shun-Xing Li, Feng-Ying Zheng, Shu-Jie Cai and Tian-Shou Cai, Determination of mercury and selenium in herbal *medicines* and hair by using a nanometer TiO<sub>2</sub>-coated quartz tube atomizer and hydride generation atomic absorption spectrometry, *Journal of Hazardous Materials*, Vol. 189, pp. 609-613 (2011)
4. J. Liu, Y. Li, S. Arumugam, J. Tudor and S. Beeby, Investigation of Low Temperature Processed Titanium Dioxide (TiO<sub>2</sub>) Films for Printed Dye Sensitized Solar Cells (DSSCs) for Large Area Flexible Applications, *Materials Today: Proceedings*, Vol.5, pp. 13846-13854 (2018)
5. Bruna Andressa Bregadiollia, Silvia Leticia Fernandes and Carlos Frederico de Oliveira Graeff, Easy and Fast Preparation of TiO<sub>2</sub> - based Nanostructures Using Microwave Assisted Hydrothermal Synthesis, *Materials Research*, Vol 20, pp. 912-919 (2017)
6. Z. Abidin, M.A. Alim, R. Saidur, M.R. Islam, W. Rashmi, S. Mekhilef and A. Wadi, Solar energy harvesting with the application of nanotechnology, *Renewable and Sustainable Energy Reviews*, Vol. 26, pp. 837-852 (2013)
7. Natividad Castro-Alarcón, José Luis Herrera-Arizmendi, Luis Alberto Marroquín-Cardena, Iris Paola Guzmán-Guzmán, Armando Pérez-Centeno and Miguel Ángel Santana-Aranda, Antibacterial activity of nanoparticles of titanium dioxide, intrinsic and doped with indium and iron, *Microbiology Research International*, Vol. 4, pp. 55-62 (2016)
8. C. Han, J. Andersen, V. Likodimos, P. Falaras, J. Linkugel and D.D. Dionysiou, The effect of solvent in the sol-gel synthesis of visible light-activated, sulfur-doped TiO<sub>2</sub> nanostructured porous films for water treatment, *Catal. Today*, Vol. 224, pp. 132-139 (2014)
9. Gema Cabello, Rogério A. Davoglio and Ernesto C. Pereira, Microwave-assisted synthesis of anatase-TiO<sub>2</sub> nanoparticles with catalytic activity in oxygen reduction, *Journal of Electroanalytical Chemistry*, Vol. 794, pp.36-42 (2017)

10. R. Mechiakh, N. Ben Sedrine, J. Ben Naceur, and R. Chtourou, Elaboration and characterization of nanocrystalline TiO<sub>2</sub> thin films prepared by sol-gel dip-coating, *Surf.Coatings Technol.* Vol. 206, pp. 243–249 (2011).

11. Areeya Aeimbhu, Effect of calcination temperature on morphology, wettability and anatase/rutile phase ratio of titanium dioxide nanotube arrays, *Materialstoday Proceeding*, Vol.5, pp. 14950-14954 (2018)

12. Dan Yang, Fengmei Cheng, Jidong Zhang, and Haidong Li, Influence of annealing temperature on morphologies and crystallinity of pure and blended diketopyrrolopyrrole - containing oligothiophene thin films, *Thin Solid Films*, Vol.645, pp. 209-214 (2018)

13. P. Elangovan and A. John Peter, Size dependent effective band gap, optical, absorption coefficients and refractive index changes in a wide ZnS/Zn<sub>1-x</sub>Mg<sub>x</sub>S strained quantum well, *Physica B: Condensed Matter*, Vol. 407, pp. 2578-2583 (2012)